Scanning-tunneling-microscope imaging of clean and alkali-metal-covered Cu(110) and Au(110) surfaces

G. Doyen, D. Drakova,* J. V. Barth, R. Schuster, T. Gritsch,† R. J. Behm,‡ and G. Ertl
Fritz-Haber-Institut der Max-Planck-Gesellschaft, Faradayweg 4-6, D-1000 Berlin 33, Federal Republic of Germany
(Received 11 September 1992; revised manuscript received 31 March 1993)

A combined experimental and theoretical study of the scanning-tunneling-miscroscope (STM) imaging properties of clean and alkali-metal covered Cu(110) and Au(110) surfaces is presented. The clean surfaces are imaged in the STM experiments as parallel strings of Cu or Au atoms, respectively, which represent the close-packed rows in the topmost layer. For the (1×2) missing-row reconstructed Au(110) surface the corrugation amplitude of the reconstruction shows a maximum as a function of tip-sample distance. On the Cu(110) surface, which does not reconstruct spontaneously in its clean state, adsorbed alkali-metal atoms (K, Cs) induce a missing-row reconstruction with the missing substrate metal rows running along the densely packed [1$\bar{1}$0] direction. On both surfaces, adatoms are located in the missing-row furrows. The alkali atoms are usually not visible in the STM picture but, rather, images are obtained typical for the reconstructed metal substrate. For certain tunneling conditions, image inversion is observed. K-covered Au(110)-(1×2) and Cu(110)-(1×2) surfaces exhibit distinct corrugation maxima similar to the clean Au(110)-(1×2) surface, if the tip-sample distance is varied. A theory of scanning-tunneling microscopy is applied that accounts for a realistic treatment of the electronic structure of the sample surface. The tunnel current is evaluated using a Green-function technique. In the theory, adsorbed potassium atoms appear transparent on Cu(110) because they substitute for sample metal atoms and are embedded in the first layer of Cu atoms. Therefore, the 4*s* resonance is centered energetically well below the Fermi level and has only a small spectral weight at the Fermi level. The corrugation maximum and the image inversion are found to be a consequence of the tip-sample interaction.

I. INTRODUCTION

The scanning-tunneling-microscope (STM) imaging process of clean metal surfaces is still under controversial discussion. Sometimes the main features of the STM images can be explained by the simple model proposed by Tersoff and Hamann,[1] which predicts that the tunneling tip follows contours of constant local density of states (LDOS) at the Fermi level (E_F) of the sample. The observation of an atomic corrugation on close-packed metal surfaces showed, however, that a more detailed modeling of the STM is necessary to understand the imaging process. This phenomenon has been studied in various theoretical investigations and tip-sample interaction is believed to play an important role.[2–4]

Many STM studies were performed during the past decade, investigating adsorption processes on metal surfaces.[5] It was shown, for instance, that it is possible to visualize single localized Xe atoms on Ni(110) at 4 K. The Xe atoms were imaged as 1.6-Å-high protrusions, and this phenomenon was attributed to the locally enhanced LDOS at E_F near the adsorbed Xe (Ref. 6) due to the unoccupied Xe 6*s* resonance level. Adsorbed oxygen atoms on Ni(001) are imaged as depressions (0.3 Å deep).[7] Within the O/Cu(110)-(2×1) system Cu-O strings appeared as protrusions or as indentations, depending on STM tip and tunneling conditions.[8] Similar observations were made for single C atoms adsorbed on Al(111).[9]

A STM theory gave the result that single alkali-metal atoms adsorbed on jellium are imaged as protrusions in STM.[10] In recent experiments, however, it was found that even in the nuclei of a (1×2) missing-row structure of Cu(110) (where the K atoms are localized) the potassium atoms are usually transparent in the STM imaging process.[11,12] This is not necessarily a contradiction as the results of the present work will demonstrate.

In this paper the STM imaging of a clean and potassium-covered Cu(110) surface will be discussed by comparing experimental results with theoretical calculations. A problem for this comparison is that the geometrical shape and the chemical composition of the apex of the tip used in experiment is unknown. Therefore the tip was modeled in a very simple way for the theoretical calculations (cf. Sec. II B) and an overall quantitative agreement between theory and experiment cannot be expected. The qualitative aspects of the imaging properties are, however, well reproduced. Experimental data are also presented for a clean and alkali-metal-covered Au(110) surface. The results are qualitatively similar to those obtained for Cu(110) suggesting the same physics of the imaging process.

Section II describes the experimental and theoretical methods. Section III presents the results for clean metal surfaces and Sec. IV those for the alkali-metal-covered surfaces. Section V summarizes the conclusions.

II. METHODS OF INVESTIGATION

A. Experiment

The experiments were performed with a pocket-size-type STM,[13] mounted in a UHV chamber with a base

pressure of 10^{-10} mbar, equipped with low-energy electron diffraction (LEED), Auger electron spectroscopy (AES), and sputter facilities. The Cu(110) and Au(110) single-crystal samples were cleaned by cycles of Ar sputtering (beam current 3 μA/cm^2; energy 500 eV; 20 min) and annealing to 1000 K until no impurities could be detected by AES and STM and the LEED patterns showed a sharp (1×1) or (1×2) pattern, respectively. Alkali-metal atoms were evaporated from commercial SAES getter sources. The alkali-metal coverages were monitored with AES. The K coverage was calibrated from the saturated K/Au(110)-c(2×2) structure with a coverage of 0.5 monolayers [ML; 1 ML corresponds to 1 alkali-metal atom per substrate atom of the (1×1) Au(110) surface].[14,15] The Cs coverage was calibrated in accordance with the formation of a well-ordered (1×2) structure on Cu(110) at $\Theta=0.2$ ML.[16] All STM measurements were performed in the constant current mode at room temperature. No filtering procedures were applied to the STM data presented here.

B. Description of the theoretical method

A theory of the scanning-tunneling microscope is applied which uses a scattering theoretical approach to calculate the current beyond perturbation theory. The method allows a realistic description of the sample surfaces. The latter are built of muffin-tin potentials accounting for the atomic and electronic structure including the d electrons. The other electrode carrying the tip atom is a planar free-electron metal surface. The potential of the tip atom is of Gaussian shape and supports an s-type bound-state resonance. Details of the theoretical formalism can be found in recent publications.[17,18,2,19]

1. Tunneling as a scattering process

In the single-particle picture the tunneling current can be viewed as a scattering process where an electron incident from the interior of the tip metal scatters at the barrier and has a certain probability of penetrating into the sample surface. The total Hamiltonian is of the form

$$H=H^0+V^{\rm tip} . \tag{1}$$

The scattering process is described by a wave function $|i+\rangle$ which is an eigenfunction of the total Hamiltonian including the tip potential $V^{\rm tip}$. i indicates the incoming momentum of the electron inside the tip electrode. When measuring the current, the scattered electron with final outgoing momentum f (after the electron has passed through the sample) is detected in the wave function $|f\rangle$, which does not experience the potential $V^{\rm tip}$ in the barrier region. This means that $|f\rangle$ has to be an eigenstate of the Hamiltonian H^0 satisfying an outgoing scattering boundary conditions. The transition matrix element for the tunneling process has the form

$$\langle f|V^{\rm tip}|i+\rangle=V_{fi}+V_{f\alpha}G_{\alpha\alpha}V_{\alpha i} . \tag{2}$$

α indicates a Gaussian basis function which characterizes the tip atom. The important task is to evaluate the exact Green function $G_{\alpha\alpha}$ in the tip region.

2. Local charge density at the Fermi level and tunnel current

The current is the electron charge e times the number of electrons which tunnel per unit time. It can be written in the form[19]

$$J=\frac{4e\pi}{\hbar}\sum_{f,i}|\langle f|V^{\rm tip}|i+\rangle|^2\,\delta(E_f-E_i) . \tag{3}$$

Using the form equation (2) of the transition matrix element in Eq. (3) then yields an expression for the tunnel current which contains quantities that are easily accessible to physical interpretation.

$$J=\frac{2\pi e}{\hbar}\frac{1}{\Delta E}\mathcal{S}^{\rm tip}_{\alpha\alpha}\mathcal{S}^{\rm cap}_{\alpha\alpha}V^2_{\alpha\alpha} \tag{4}$$

with

$$\mathcal{S}^{\rm tip}_{\alpha\alpha}=\sum_i\langle\alpha|i+\rangle\langle i+|\alpha\rangle , \tag{5}$$

$$\mathcal{S}^{\rm cap}_{\alpha\alpha}=\sum_f\langle\alpha|f\rangle\langle f|\alpha\rangle . \tag{6}$$

The summations in Eqs. (5) and (6) run over states in the energy range ΔE between the two Fermi levels. In this paper we consider the limit of an infinitesimally small applied voltage, i.e., ΔE tending to zero. For metal surfaces the imaging properties do not depend significantly on the bias and therefore the voltage dependence is not investigated in this publication. $V_{\alpha\alpha}$ is a matrix element of the tip potential. $\mathcal{S}^{\rm tip}_{\alpha\alpha}$ is a matrix element of the projection operator $\sum_i|i+\rangle\langle i+|$ in the localized basis set. The projection is on the eigenfunctions of the total Hamiltonian with boundary conditions corresponding to incident waves from the tip side. $\mathcal{S}^{\rm tip}_{\alpha\alpha}$ is the projection of the local function $|\alpha\rangle$ in the barrier on those exact scattering eigenstates that are generated by incident waves running towards the sample surface and will be termed TIP-LOD (tip-projected local density).

$\mathcal{S}^{\rm cap}_{\alpha\alpha}$ is the corresponding projection on the eigenstates of the system without the tip atom, which resembles a capacitor of two plane electrodes. These are eigenfunctions of H^0 with boundary conditions corresponding to Bloch waves $|f\rangle$ parallel to the electrodes propagating away from the interface. The diagonal matrix elements represent the electron density of the corresponding wave functions at the Fermi level averaged over the tip region. $\mathcal{S}^{\rm cap}_{\alpha\alpha}$ is the projection of the local state on eigenfunctions of the two-electrode system without the tip atom and is called CAP-LOD (capacitor-projected local density). It may be interpreted as a partial local charge density at the Fermi level of the unperturbed two-electrode system (sample plus free-electron electrode).

The localized function $|\alpha\rangle$ in the barrier is chosen to define the tip region and shape, i.e., the region in position space, where the tip potential acts. Hence, the meaning of the capacitor- and tip-projected local electron densities is just the electron density at the Fermi level projected onto the region, where the tip potential is effective for the system without and with the tip. The CAP-LOD's thus include information about the electron structure of the sample, whereas the additional information gained from

TIP-LOD's can be attributed to the tip-sample interaction. This means that the comparison of the tunnel current contrast with the variations of CAP-LOD and TIP-LOD yields information about the influence of tip-sample interactions.

3. The model potential

The potential in the interior of the tip metal is kept constant which means that the tip base is represented by a free-electron metal. The work function and the energetic width of the occupied free-electron states are chosen to correspond to Al(111) ($\phi_{\mathrm{Al(111)}}=4.26$ eV, $V_0=11.7$ eV). The region of flat potential inside the tip electrode is separated from the semi-infinite sample by a square barrier, which is positioned at the rim of the first-layer muffin-tin spheres.

The muffin-tin potentials for the Cu and K atoms are taken from the self-consistent bulk calculations of Moruzzi *et al.*[20] The Cu Fermi level is at 9.35 eV relative to the bottom of the *sp* band.[20] The work function of Cu(110) is 4.5 eV (Ref. 21) so that for the two-electrode system (capacitor) the barrier height as seen from the sample side is 13.85 eV relative to the muffin tin zero. For the potassium-covered surface the work function was assumed to be 2.3 eV.[22] The kinetic energy of the incident electron is always 11.68 eV.

A localized attractive potential is introduced inside the barrier, which models the tip. As the microscopic structure of the tip is unknown, we decided for the present study to assume a Gaussian shape, which is computationally convenient. The Gaussian representing the tip atom is centered at 1.1 Å in front of the tip electrode and has a lateral radial range of ca. 1.7 Å parallel to the surface (decay $\alpha=0.1$ bohr^{-2}). The expectation value of the local tip potential in the region of the Gaussian is -13.6 eV.

III. IMAGING THE CLEAN METAL SURFACES

A. Cu(110)

An experimental STM image of the clean Cu(110) surface is reproduced in Fig. 1. Individual strings consisting of Cu atoms running along the close-packed [1$\bar{1}$0] direction are clearly resolved with a next-nearest-neighbor distance of 3.6 Å. The average corrugation amplitude of the atom rows amounts to 0.2 Å, as can be seen from the STM contour line in this figure. A slightly smaller corrugation amplitude of 0.14 Å was reported for this surface in an earlier STM study.[23] In this work it was furthermore shown that it is possible to resolve the individual Cu atoms within the [1$\bar{1}$0] strings. In a helium atom scattering (HAS) study, a corrugation amplitude of 0.09 Å along the [001] direction was reported.[24]

Figure 2(a) shows the calculated variation of the tunnel current across the Cu(110) surface at a constant tip height of 3.9 Å above the first layer of Cu atoms. For the sake of clarity we point out that all theoretical STM images were calculated at constant tip height in contrast to the experimental data, which were recorded in the constant current mode. The empty circles in Fig. 2(a) indicate the positions of the Cu atoms in the surface unit cell. The close-packed rows of Cu atoms are imaged as bright stripes. Cu atoms in the second layer are not visible. The maximum variation of the tunnel current is approximately 7% which corresponds to a corrugation amplitude of roughly 0.04 Å (cf. Sec. III C). This is relatively small compared to the experimental values and reflects a general problem of STM theories in predicting the large corrugations observed in experiment for close-packed metal surfaces.[2]

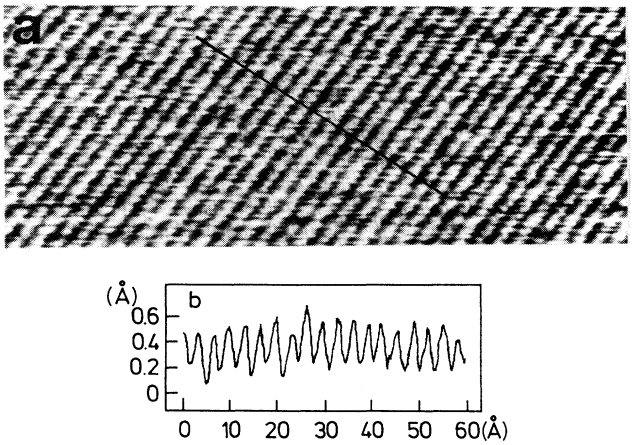

FIG. 1. (a) Experimental STM image of the clean Cu(110) surface. (b) STM contour line along the marked line in (a).

The variation of CAP-LOD and TIP-LOD across the Cu(110) surface at a constant height of 3.9 Å above the first layer of Cu atoms is depicted in Figs. 2(b) and 2(c). The maximum variation is 8% for CAP-LOD and 2% for TIP-LOD. The close-packed rows of Cu atoms are visualized as bright stripes in CAP-LOD. In TIP-LOD the Cu atoms in the first layer appear as dark spots whereas the Cu atoms in the second layer are bright spots. This indicates that the tip-sample interaction is larger in the center of the surface unit cell (due to the larger number of adjacent sample atoms) than for a tip placed above a Cu atom in the first layer. The tip-sample interaction leads to the formation of bonding and antibonding states with the antibonding states increasing the local density of states near the Fermi level. This behavior of the TIP-LOD decreases the corrugation in the [001] direction of the tunnel current at closer distances. At 3.9 Å tip-sample distance the variation in TIP-LOD is too small so that essentially an image of the local sample charge density at the Fermi level averaged over the region of the tip orbital is obtained in STM. This is reflected in the fact that the variation of the total tunnel current is essentially the same as the variation of CAP-LOD.

B. Reconstructed surfaces

1. Cu(110)-(1×2)

A clean reconstructed Cu(110) surface has not been observed in experiment. We constructed a theoretical mod-

el of such a surface in order to separate the influence of adsorbed potassium on the STM image. Figure 2(d) shows the variation of the tunnel current across the Cu(110)-(1×2) missing-row reconstructed surface at a constant height of 3.9 Å above the first layer of Cu atoms. The maximum variation is approximately 30%, which corresponds to a corrugation amplitude of roughly 0.3 Å compared to a maximal corrugation amplitude of 1 Å observed in experiment for the Au(110)-(1×2) missing-row reconstructed surface (cf. Sec. III C). The closed-packed rows of Cu atoms again form regions of large tunnel current. The sites where the Cu atoms have been removed to form the missing row appear as holes.

For this surface the maximum variation is 30% for CAP-LOD and 4% for TIP-LOD. In marked difference to the unreconstructed Cu(110) surface, the close-packed

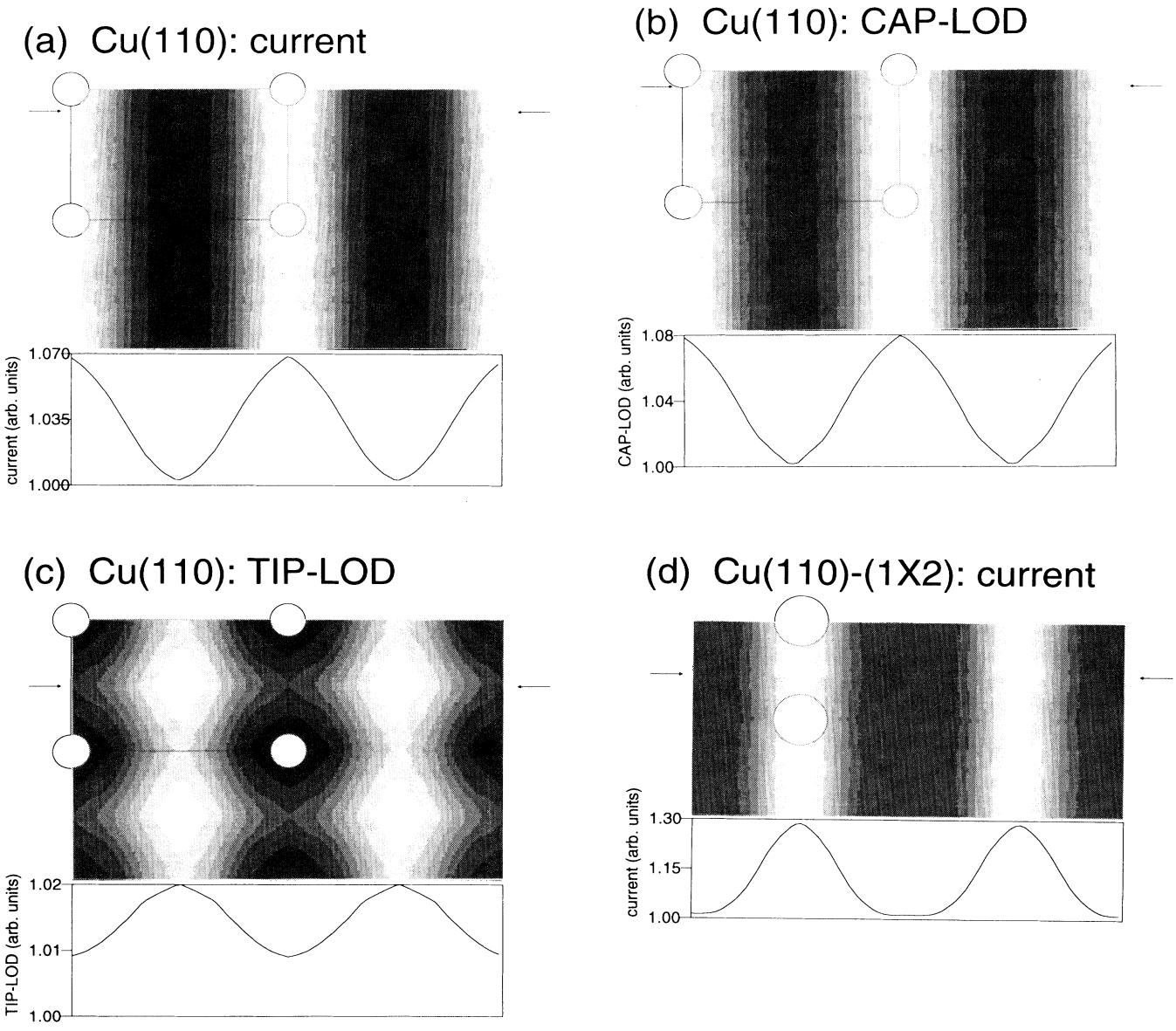

FIG. 2. (a) Gray scale representation of the calculated variation of the total tunneling current parallel to a Cu(110) surface for a tip-sample separation of 3.9 Å. The maximal variation is 7%, as can be seen from the contour line at the bottom of the figure which gives the current along the line connecting the two arrows. The empty circles indicate Cu atoms in the first layer. (b) Lateral variation of the capacitor-projected local density at the Fermi level (CAP-LOD) for Cu(110) at a tip-sample separation of 3.9 Å. (c) Lateral variation of the tip-projected local density at the Fermi level (TIP-LOD) for Cu(110) at a tip-sample separation of 3.9 Å. (d) Variation of the total tunnel current parallel to a Cu(110)-(1×2) missing-row reconstructed surface at a constant height of 3.9 Å above the first layer of Cu atoms. The maximum variation is approximately 30%. The empty circles indicate the positions of the Cu atoms in the surface unit cell.

rows of Cu atoms appear as bright stripes in CAP-LOD *and* TIP-LOD. At 3.9 Å tip-sample distance the variation in TIP-LOD is, however, too small so that again essentially an image of the local sample charge density averaged over the region of the tip orbital is obtained in STM. Qualitatively our theoretical results for Cu(110)-(1×2) are in close analogy to previous experimental and theoretical STM investigations for Au(110)-(1×2).[1,25–28]

2. *Au(110)-(1×2)*

This surface has only been studied experimentally. The clean Au(110) surface exhibits a (1×2) missing-row reconstruction, where every second $[1\bar{1}0]$ row of atoms is absent.[29] The Au(110)-(1×2) reconstructed surface has been studied extensively by STM during the past few years.[25–28] The experimentally found corrugation amplitude in the [001] direction varied between 0.3 and 1 Å. The STM images were explained by a simple model, where it was shown that a spherical tunneling tip follows contours of constant LDOS at E_F.[1]

C. Distance dependence of the corrugation amplitude

Figure 3 shows the calculated corrugation amplitude (i.e., the maximal lateral variation in the perpendicular tip excursion for constant tunnel current) as a function of tip-sample separation for Cu(110)-(1×1). Starting from large distances the corrugation amplitude increases and reaches a maximum at approximately 3.7 Å. At closer distances it decreases and changes to negative values at 2.7 Å, which indicates image inversion. The behavior at smaller distances is due to the tip-sample interaction, which is largest in the center of the unit cell because of the larger number of sample atoms involved in the interaction. Tip-sample interaction increases the local charge density at the Fermi level due to the formation of bonding and antibonding states. The antibonding states are higher in energy and spread over a broader energy range but having a significant spectral weight at the Fermi level. This enhancement of the spectral weight at the Fermi level becomes larger with decreasing tip-sample interaction and it is more pronounced for the lateral tip position in the center of the unit cell. More details about this mechanism can be found in Ref. 2 where it was studied for close-packed surfaces of Al and Pd.

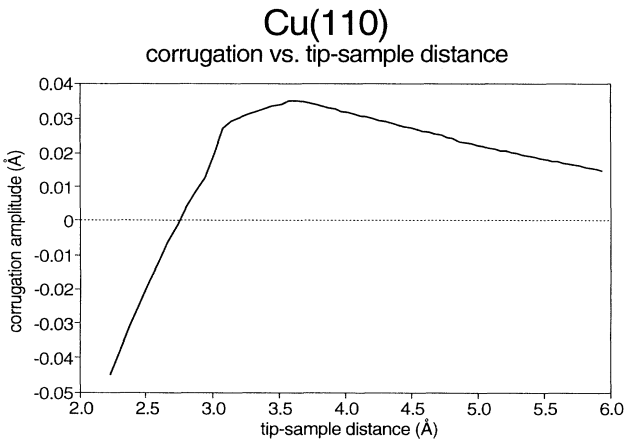

FIG. 3. Calculated corrugation amplitude (i.e., maximal lateral variation in the perpendicular tip excursion for constant tunnel current) as a function of tip-sample separation for Cu(110).

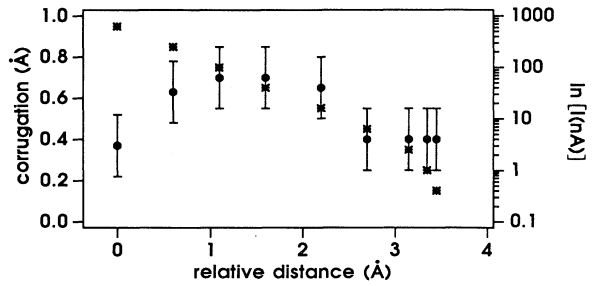

FIG. 4. Experimental corrugation amplitude of the clean Au(110)-(1×2) missing-row structure (dots, left-hand-side axis) and tunneling currents (crosses, right-hand-side axis) at a constant tunneling voltage of −550 mV vs the relative tip-sample distance.

A direct test for the theoretical considerations is the measurement of the dependence of the corrugation amplitude of the (1×2) missing-row structure on the tip-sample distance. Figure 4 shows the corrugation of the clean Au(110) missing-row structure, obtained by STM at a constant tunneling voltage of $U_T = -550$ mV versus the relative tip-sample distance (only change of distance can be measured, zero distance has been chosen arbitrarily). In the diagram a maximum of the corrugation amplitude of 0.7 Å at 100 nA tunneling current can be seen. (It should be noted that maximal corrugation amplitudes of 1 Å were observed on this surface.) For lower as well as for higher currents the corrugation amplitude decreases. Such effects are typically observed on reconstructed corrugated metal surfaces and were likewise seen on the clean Pt(110)-(1×2) missing-row reconstructed surface[28] and on the reconstructed Au(001)-(5×20) (Ref. 30) surfaces.

Figure 5 displays the calculated corrugation amplitude

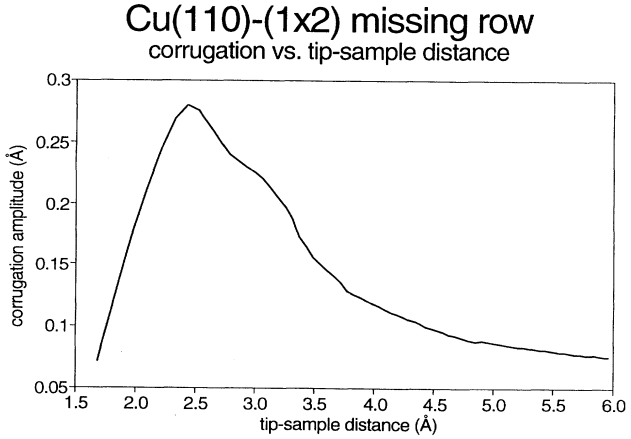

FIG. 5. Calculated corrugation amplitude as a function of tip-sample separation for the (1×2) missing-row reconstructed Cu(110) surface.

as a function of tip-sample separation for the 1×2 missing-row reconstructed Cu(110) surface. The qualitative behavior is similar to that of the nonreconstructed Cu(110) surface, but the corrugation amplitude is larger and it reaches its maximum at closer distances (at approximately 2.3 Å). If the tip is positioned above the missing row, it has to penetrate deeper into the surface in order to experience a significant tip-sample interaction. Eventually this interaction becomes stronger here than on top of the Cu rows, but this happens at rather close distances. The shape of the theoretical curve of Fig. 5 resembles closely the corresponding experimental curve for Au(110)-(1×2) shown in Fig. 4. A change of one order of magnitude in the tunnel current in Fig. 4 corresponds roughly to a variation of the tip-sample distance of 1 Å. A theoretical treatment of the Au surface is not included in this work, because relativistic effects have to be accounted for, which is not feasible at the present state of the theory.

D. Apparent barrier height

The described behavior of the tunnel current with distance is also reflected in the theoretical apparent barrier heights, which are displayed in Fig. 6. The apparent barrier height is proportional to the square of the logarithmic derivative of the tunnel current with respect to the tip-sample separation.[19] At large distances of the tip it should become equal to the work function of the sample surface, at intermediate distances values larger than the work function are possible;[17,31] at close distances this quantity need not directly be connected to the local potential in the barrier. The apparent barrier height derived from the tunnel current might be compared to the square of the logarithmic derivative of the charge density, which will be termed the charge-density-derived apparent barrier height. At large distances the apparent barrier heights derived from either the tunnel current or the charge density should be equal. This is the case for the unreconstructed Cu(110) surface as can be seen in Fig. 6(a). At closer distances the current-derived apparent barrier height is larger than the charge-density-derived apparent barrier height, because the tip-sample interaction leads to a more strongly increasing current with decreasing tip-sample distance than would be obtained in perturbation theory from an estimation of the charge density.

For the missing-row reconstructed Cu(110)-(1×2) surface the (current-derived) apparent barrier height [depicted in Fig. 6(b)] is, at separations where tip-sample interaction is not yet effective, smaller above the missing rows. The reason is that above the missing rows the charge density saturates at a smaller value and therefore (starting from zero at infinity) it flattens off at larger distances than atop the Cu rows. When tip-sample interaction sets in, the current is increased more strongly above the missing rows and therefore the apparent barrier height never acquires very small values and at 2.5 Å it becomes larger than above the Cu rows. At close distances the apparent barrier height is larger for the tunnel current than for the CAP-LOD [similar to Cu(110) as shown in Fig. 6(a)], because tip-sample interaction sets in and the tunnel current saturates more slowly than the local charge density. The CAP-LOD derived barrier height would be the result in the Tersoff-Hamann approximation.

To illustrate the influence of the tip-sample interaction Fig. 7 displays on a logarithmic scale the distance depen-

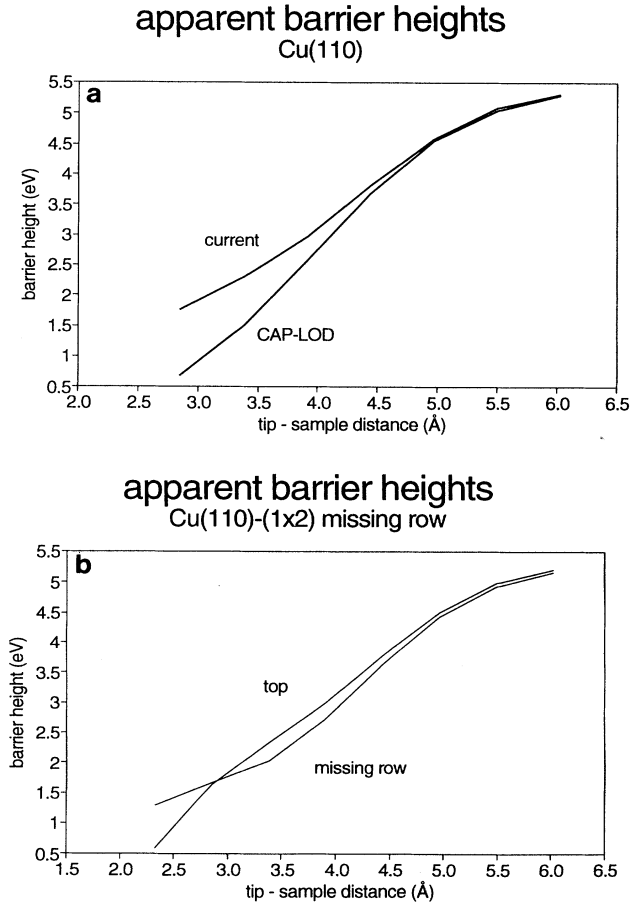

FIG. 6. Calculated apparent barrier heights for (a) Cu(110) and (b) Cu(110)-(1×2).

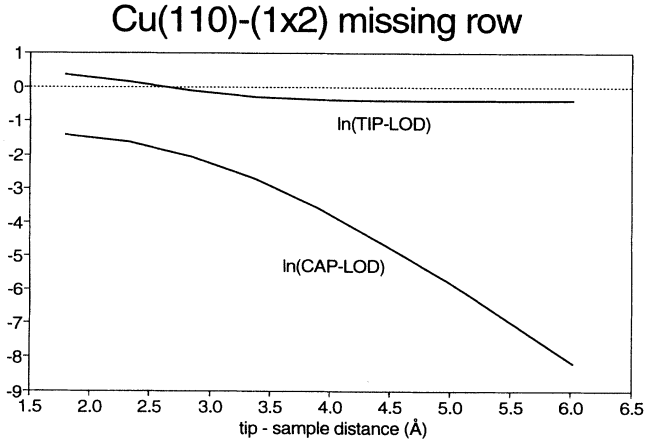

FIG. 7. Distance dependence of the logarithms of CAP-LOD and TIP-LOD for Cu(110)-(1×2).

dence of CAP-LOD and TIP-LOD for Cu(110)-(1×2) for the tip placed above the row of Cu atoms. At large distances CAP-LOD, which characterizes the local sample charge density at the Fermi level, decreases exponentially. TIP-LOD characterizes the local charge density at the Fermi level of the tip in interaction with the sample and therefore at large distances tends to the constant value characteristic of the noninteracting tip. At closer distances CAP-LOD levels off slowly, because the tip orbital now not only probes the exponentially decaying tails of the sample wave functions, but also interior parts of the sample electronic structure. TIP-LOD increases at closer distances (≤ 4 Å) when the tip-sample interaction starts to become important. Therefore the tunnel current levels off more slowly than the local sample charge density (CAP-LOD).

IV. IMAGING OF ALKALI-METAL-COVERED Cu(110) AND Au(110) SURFACES

Alkali-metal adsorption on the (110) faces of the 3*d* and 4*d* transition-metal surfaces of Ni, Cu, Pd, and Ag induces missing-row-type reconstructions.[32] As shown in detail for K/Cu(110), this reconstruction proceeds at low coverages ($\Theta \leq 0.05$) via the formation of homogeneously spread nuclei of a reconstruction, where single alkali-metal atoms have removed two or three Cu atoms out of the [1$\bar{1}$0] rows of the Cu(110) surface and locate themselves in the resulting hole.[11,12] With increasing coverage these nuclei arrange to (1×3) and (1×2) missing-row-type structures, where every third or every second Cu [1$\bar{1}$0] row has been removed, respectively. Cs and Na adsorption on Cu(110) were shown to form structures analogous to that of K/Cu(110).[33,34] A structural model of the local reconstruction is given in Fig. 8. Generally in these investigations the alkali-metal atoms themselves are not directly identifiable in the STM image except for the substrate reconstructions they induce.

A. Alkali-metal adsorption on Cu(110)

Figure 9 shows STM images of the local reconstruction of Cs/Cu(110) at $\Theta=0.05$ with different tip conditions. In the upper part of Fig. 9 the cesium-induced local reconstructions are imaged as small holes, approximately 0.3 Å deep. After a sudden change of the tip (perhaps by crashing against the defect in the lower right part of the image) these holes were imaged as protrusions with a height of up to 1 Å. Since the tip base had to move 3 Å closer to the surface while the tip modification occurred, a structural rearrangement of the outermost atoms of the tunneling tip presumably has taken place. In the upper part of the second image Fig. 9(b), which was taken of exactly the same area, the tip has stabilized slightly. [Slightly changed monoatomic steps can be observed, because at room temperature the steps on the Cu(110) surface are mobile, as shown in Ref. 35.] At this point the tip changes again. It retracts by about 1.5 Å and the nuclei of the reconstruction are imaged as indentations, which can be nicely seen in the lower part, where, after a second tip change, the tip has further stabilized. Such changes of the imaging of the cesium-induced reconstructions on Cu(110) occurred at all investigated coverages up to $\Theta=0.3$ ML and were also observed occasionally for the K/Cu(110) system.

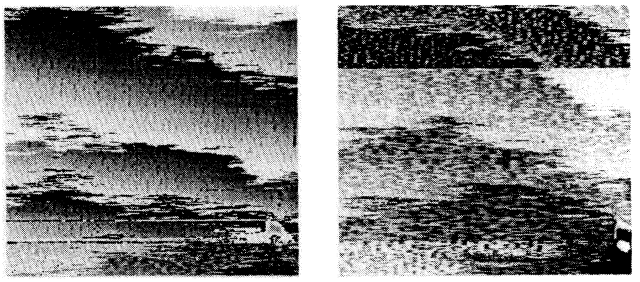

FIG. 9. STM images of the local reconstruction of Cs/Cu(110) at $\Theta=0.05$ in different imaging modes of the tip. Both images show the same surface area. In the lower part of the left image and in the upper part of the right image the state of the tip changed.

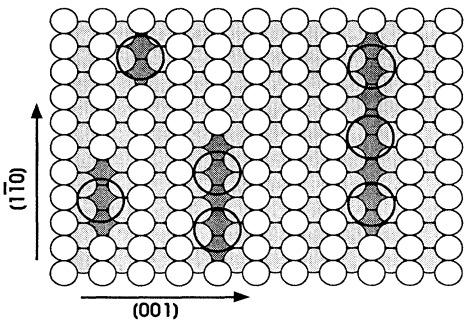

FIG. 8. Structure model for the reconstruction nuclei of K/Cu(110). Large open circles: K atoms; small white (gray and dark) circles; Cu atoms in the first (second and third) layer.

Figure 10 shows an image of the (1×2) missing-row reconstructed K/Cu(110) surface at $\Theta=0.20$ ML. It can be assumed that step edges, running along the [1$\bar{1}$0] direction must be formed by Cu [1$\bar{1}$0] rows and not by the rather mobile alkali-metal atoms. [The mobility of the K atoms in the (1×2) troughs was deduced from LEED experiments. Only at lower temperatures do the K atoms form ordered structures in the troughs, which are not observed at room temperature.[16]] Hence from the imaging of these step edges as bright protrusions it is assumed that the Cu[1$\bar{1}$0] rows are imaged as protrusions and the potassium-filled missing-row troughs as indentations, respectively. The troughs in the STM image are 0.5 Å deep. Similar observations were made with K/Cu(110)-(1×3), where the K-filled missing-row troughs were imaged as depressions with STM.[11] A model of the (1×2) missing-row structure with adsorbed potassium is reproduced in Fig. 10(b).

Turning now to the theoretical simulations, Fig. 11(a) shows the calculated variation of the tunnel current across the K-covered Cu(110)-(1×2) missing-row reconstructed surface at a constant height of 3.9 Å above the first layer of K atoms. A close-packed row of K atoms has been inserted in the missing row such that the

muffin-tin spheres of the atoms touch. This means that the center of the K atoms is 1.6 Å above the first layer of Cu atoms. The coverage is $\Theta=0.5$ ML. The maximum variation of the tunnel current is approximately 30%. The circles indicate now the position of the K atoms in the surface unit cell. The close-packed rows of Cu atoms are imaged as bright stripes. The regions where the K atoms have replaced the Cu atoms are imaged as deep troughs.

In Figs. 11(b) and 11(c), we see the variation of CAP-LOD and TIP-LOD across the K-covered Cu(110)-(1×2) missing-row reconstructed surface at a constant height of 3.9 Å above the first layer of K atoms. The maximum variation is approximately 30% for CAP-LOD, for TIP-LOD it is 8%. The empty circles indicate the position of the K atoms in the surface unit cell. The closed-packed rows of Cu atoms appear as bright stripes in CAP-LOD and in TIP-LOD. The TIP-LOD behavior is different from the situation for Cu(110) but similar to the (1×2) reconstructed surface without a K adlayer. The variation in TIP-LOD only very slightly amplifies the corrugation in the local sample charge density at the Fermi level as given by CAP-LOD. Therefore the corrugation is not influenced by the tip-sample interaction at that distance. The K atoms appear as faint stripes in TIP-LOD.

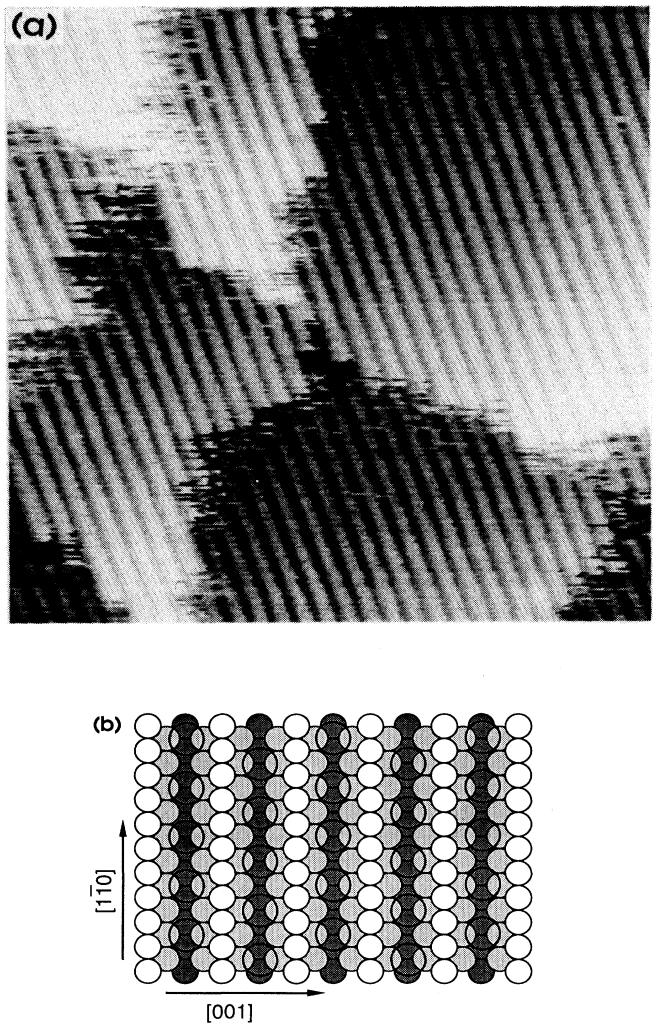

FIG. 10. (a) STM image of the (1×2) missing-row reconstructed K/Cu(110) surface at $\Theta=0.20$. (b) Model for the K-covered (1×2) structure. The symbols are identical with those in Fig. 8.

The fact that the K atoms are not seen in the STM image is obviously a consequence of the local charge density at the Fermi level, because the K atoms are not discernible in the variation of CAP-LOD. This might be understood from the work of Drakova, Doyen, and Hübner.[36] They studied the Li-induced 2*s* density of states as a function of distance between the Li atom and the Cu(100) surface. Near the equilibrium position the Li-induced local density of states at the Fermi level is high, whereas it reduces to near zero, if the Li atom penetrates into the surface. The Li atom then forms a strong chemical bond with the Cu metal, exhibiting bonding and antibonding states which are split off far from the Fermi energy.

These effects occur at larger distances for adsorbed K, because the 4*s*-valence orbital is more diffuse. In metastable deexcitation spectroscopy a 4*s*-derived resonance feature due to adsorbed K on Cu(110)-(1×2) was found to be centered 2 eV below the Fermi level,[22] which supports the present point of view. With this kind of bonding for the substitutional K adsorption on Cu(110), we gain as well an understanding of the behavior of TIP-LOD [cf. Fig. 11(c)], the charge density at the Fermi level of the interacting tip-sample system. Near the Fermi level the antibonding K-Cu states have a larger weight than the bonding ones. If the tip is in a lateral position between a Cu and a K atom, then the substrate wave function will have a node in this region and the overlap with the tip wave functions is small. Therefore the tip-sample interaction is small for this lateral position and the TIP-LOD has a minimum here [cf. Fig. 11(c)]. This minimum leads to a larger overall variation of TIP-LOD.

Our explanation for the invisibility of the K atoms in STM depends very much on the fact that the K atoms are embedded rather than adsorbed on top of a close-packed metal surface. For the latter situation the adsorbed alkali-metal atoms might very well appear as protrusions in STM.[10]

The image inversion is observed on the K/Cu(110)-(1×2) missing-row reconstructed surface at close distances (smaller than 2.5 Å) similar to what has been predicted for the clean Cu surfaces. Figure 11(d) shows the variation of the tunnel current across the K-covered Cu(110)-(1×2) missing-row reconstructed surface at a constant height of 2.3 Å above the first layer of K atoms. Compared to Fig. 11(a) the calculated STM image appears inverted at this closer distance. The maximum variation is approximately 50%. The empty circles indicate again the position of the K atoms in the surface unit cell. The rows of K atoms are imaged as bright stripes, whereas the rows of close-packed Cu atoms are imaged as deep troughs.

Figures 11(e) and 11(f) give the variation of CAP-LOD and TIP-LOD across the K-covered Cu(110)-(1×2) missing-row reconstructed surface at a constant height of

2.3 Å above the first layer of K atoms. The maximum variation is 20% for CAP-LOD and 80% for TIP-LOD. The close-packed rows of Cu atoms appear as bright stripes in CAP-LOD and as dark regions in TIP-LOD. CAP-LOD did not change qualitatively compared to 3.9-Å tip-sample separation, but for TIP-LOD the situation is completely different. The K atoms appear as bright stripes in TIP-LOD because of the strong chemical interaction between the tip and the K atoms, which adds local K-derived density of states at the Fermi level. This

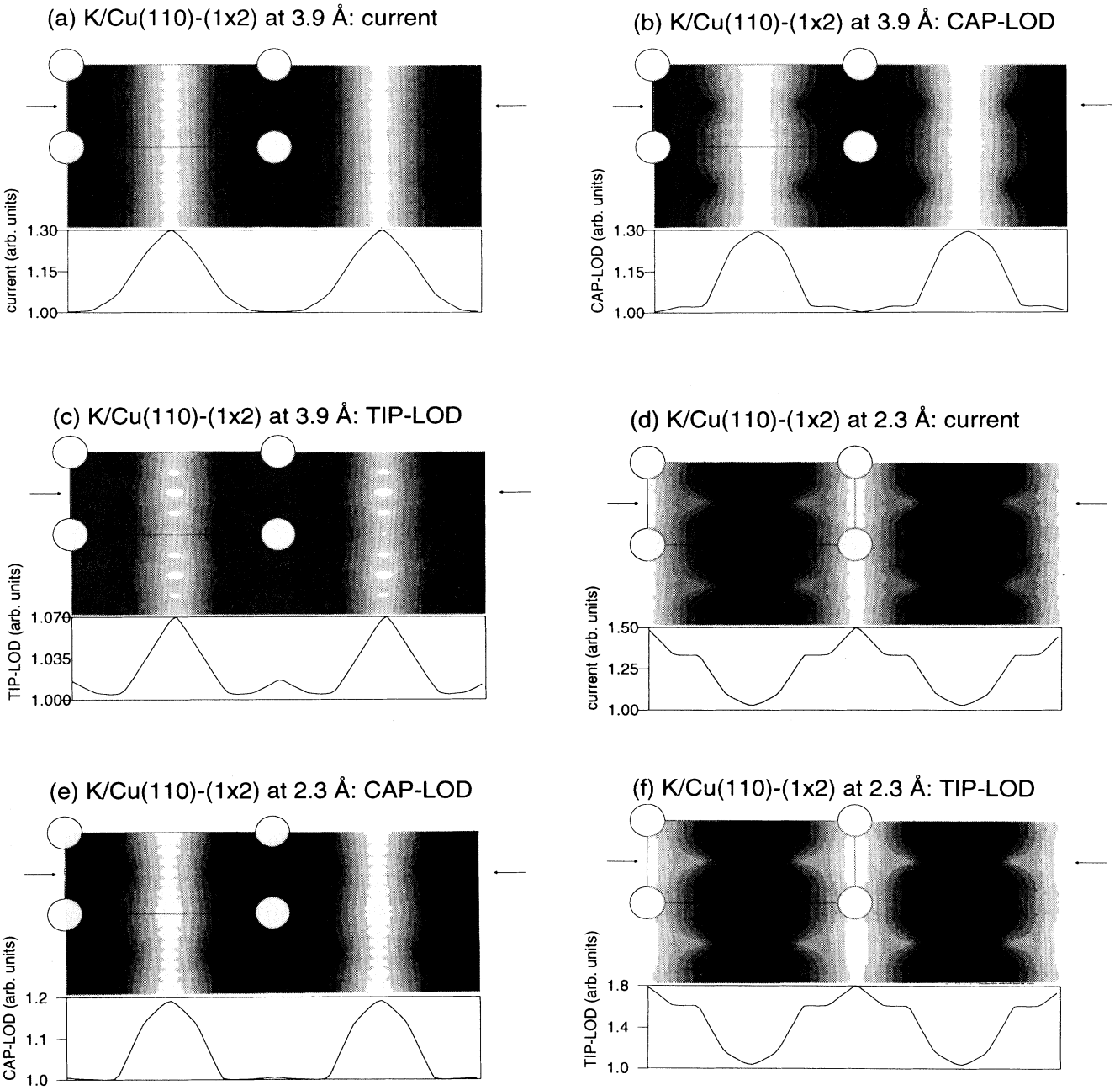

FIG. 11. (a) Calculated variation of the tunnel current across the K-covered Cu(110)-(1×2) missing-row reconstructed surface at a constant height of 3.9 Å above the first layer of K atoms. (b) Variation of CAP-LOD and (c) TIP-LOD across the K-covered Cu(110)-(1×2) missing-row reconstructed surface at a constant height of 3.9 Å above the first layer of K atoms. (d) Variation of the tunnel current across the K-covered Cu(110)-(1×2) missing-row reconstructed surface at a constant height of 2.3 Å above the first layer of K atoms. (e) Variation of CAP-LOD and (f) TIP-LOD across the K-covered Cu(110)-(1×2) missing-row reconstructed surface at a constant height of 2.3 Å above the first layer of K atoms. (The circles indicate the position of the K atoms in the surface unit cell.)

explains the image inversion. The tip-sample interaction is now strong enough so that considerable local charge rearrangement in the sample occurs and the K-Cu bond is weakened in favor of the tip-K bond.

B. Alkali-metal adsorption on Au(110)

The (1×2) missing-row structure of Au(110) is not altered after adsorption of 0.15–0.25 ML of potassium.[15] Surprisingly the STM topography of the surface in this coverage range is equivalent to that of the clean surface. This is shown in Fig. 12, where a STM image of Au(110) with a K coverage of 0.15 ML is depicted. The adsorbed K atoms do not show up here, as can be deduced from the appearance of the step edges. Furthermore, the K-K distance at this coverage amounts to approximately 9 Å along $[1\bar{1}0]$ in the reconstruction furrows, so that effects due to the individual potassium atoms should be observable in STM if they would contribute significantly to the tunnel current. The corrugation amplitude of the (1×2) structure amounts in this case to 0.8 Å, which would be a typical value also for the clean surface. The only apparent difference with respect to the K/Cu(110)-(1×2) structure, as shown in Fig. 10, is that in the Au(110) case the atomic steps appear stable and not frizzled as with Cu(110). An argument in favor of why the adsorbed K atoms are invisible might be the high mobility of the adsorbed K atoms. But even with potassium coverages ≥ 0.25 ML, where nuclei of the K-Au-$c(2\times2)$ structure are formed on Au(110) (Ref. 15) and where the K atoms are not able to move, they are usually transparent in the STM image. This is obvious from the STM image reproduced in Fig. 13(a). In this experiment 0.32 ML of potassium were deposited on Au(110). At this coverage the (1×2) missing row coexists with islands of the $c(2\times2)$ structure. A model of the nucleus of the $c(2\times2)$ structure, where the K and Au atoms locally form a mixed overlayer surrounded by (1×2) missing-row areas, is illustrated in Fig. 13(b). For the formation of the $c(2\times2)$ structure Au atoms of the $[1\bar{1}0]$ rows merely have to be displaced by 4.08 Å (the lattice constant of Au) in the [001] direction. The outermost atoms of the interrupted $[1\bar{1}0]$ strings together with the displaced Au atoms form the $c(2\times2)$ unit cell. The vacancies in the $[1\bar{1}0]$ strings are occupied by K atoms. The position of the K atoms within the $c(2\times2)$ geometry has been determined with medium energy ion scattering,[14] confirming a theoretical prediction.[37] They lie 1.1 Å above the plane of the Au surface atoms. By comparing the model with the STM image it becomes immediately apparent that the positions of the K atoms in the $c(2\times2)$ nucleus are imaged as depressions, whereas the Au atoms show up as protrusions. A full account of the STM observations of the K/Au(110) system will be given elsewhere.[38]

C. Distance dependence of the corrugation amplitude: Alkali-metal-covered Cu(110) and Au(110) surfaces

The dependence of the corrugation amplitude on the tip-sample separation of K-covered Cu(110)-(1×2) and Au(110)-(1×2) missing-row reconstructed surfaces exhibits qualitatively just the same behavior as the clean

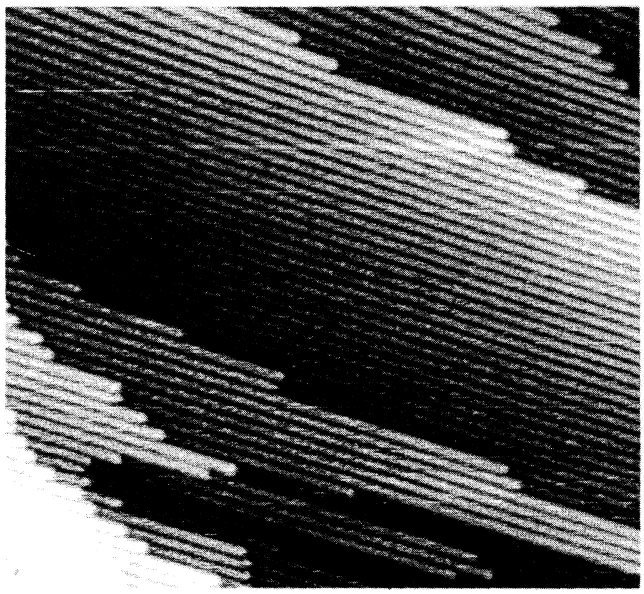

FIG. 12. STM image of Au(110)-(1×2) with a K coverage of 0.15 ML.

Au(110)-(1×2) surface. This is shown for K/Cu(110)-(1×2) at a K coverage of 0.2 ML in Fig. 14(a) (only relative distance changes can be measured, zero distance has been chosen arbitrarily). The corrugation amplitudes were obtained during one experiment, where the tunneling current was switched at a constant tunneling voltage of -790 mV. The corrugation changes shown are reversible, i.e., independent of whether the tunneling currents are lowered or enlarged during these series.

A diagram of the (1×2) corrugation amplitude of the reconstructed Au(110) surface covered with 0.25 ML of potassium at a constant tunneling voltage of -590 mV is

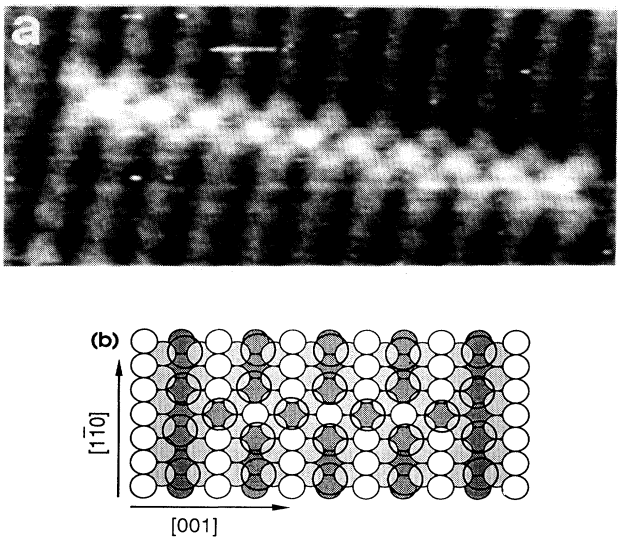

FIG. 13. (a) STM image of Au(110) with a K coverage of 0.32 ML. (b) Model of the $c(2\times2)$ nucleus for K/Au(110). For an explanation of the symbols, see Fig. 8.

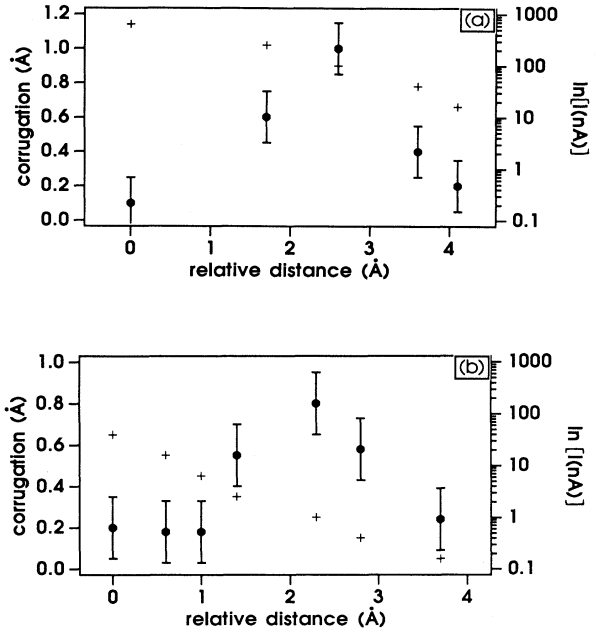

FIG. 14. Measured corrugation amplitudes (dots) and tunneling currents (crosses) vs the relative tip-sample distance: (a) for K/Cu(110)-(1×2) at a K coverage of 0.2 ML and a constant tunneling voltage of −790 mV; (b) for K/Au(110)-(1×2) at a K coverage of 0.25 ML and a constant tunneling voltage of −590 mV.

shown in Fig. 14(b). Again the dependence was reversible and no tip change occurred during the experiment. Similar with the clean Au(110)-(1×2) and the *K*-covered Cu(110)-(1×2) surface a marked maximum of the corrugation amplitude was observed.

The theoretically determined corrugation amplitude as a function of tip-sample separation for the K-induced (1×2) missing-row reconstructed Cu(110) surface is depicted in Fig. 15. Because the missing rows are now filled with K atoms, the tip-sample interaction sets in here at larger distances and the anticorrugating effect of this interaction is felt earlier. Therefore the maximum is reached already at 3.8 Å and image inversion ensues at approximately 2.5 Å. The theoretical corrugation amplitudes have been calculated for the applied voltage tending to zero. On metal surfaces no dramatic effects are to be expected as a function of the bias. Experimentally the corrugation amplitude can only be determined with an error of about 0.15 Å.

D. Apparent barrier height

The effective barrier heights for K/Cu(110) obtained from Fig. 14(a) vary between 1.5 and 2.5 eV. They have been estimated by evaluation of the retraction of the tip between subsequent steps of the tunneling current using the logarithmic derivative of the tunnel current with respect to distance. The experimental apparent barrier height is lower at higher tunneling current and increases if the tip retracts.

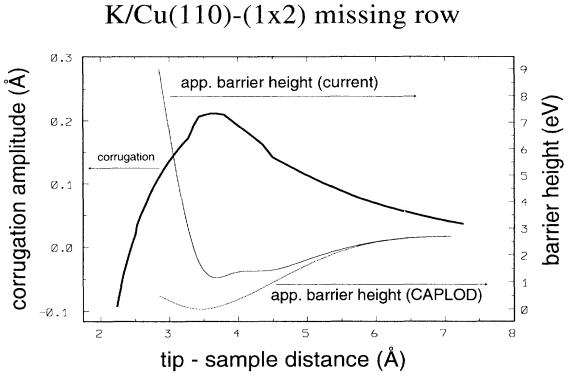

FIG. 15. Calculated corrugation amplitude as a function of tip-sample separation for the K-induced (1×2) missing-row reconstructed Cu(110) surface. Also displayed are the calculated apparent barrier heights for K/Cu(110)-(1×2) as a function of tip-sample separation.

Theoretically the extended nature of the K atoms is responsible for the far-reaching tip-sample interaction on this surface. As a consequence of this the calculated apparent barrier height (cf. Fig. 15) does not decrease to smaller values compared to the clean surfaces, although the work function is considerably smaller [2.3 eV for K/Cu(110)-(1×2), compared to 4.5 eV for the clean C(110) surface]. In fact it starts increasing again at 4 Å, when the tip-sample interaction starts dominating. The charge-density-derived apparent barrier height decreases to zero.

V. CONCLUSIONS

The two most prominent characteristics observed in STM experiments on the clean Au(110) and Cu(110) surfaces and on the K-covered (1×2) surfaces are the maximum in the corrugation amplitude of the (1×2) structures upon varying the tip-sample distance and the fact that adsorbed alkali-metal atoms often appear transparent in the images. A theoretical model with a single atom tip gives an explanation for the experimental STM observations. The maximum in the corrugation amplitude for the (1×2) reconstructed surfaces is rationalized as the result of the competing action of the corrugating effect of the charge density of the unperturbed surface and the anticorrugating influence of the tip-sample interaction. This interpretation holds both for the clean and the K-covered surfaces. It was shown that the adsorbed alkali-metal atoms do not influence the STM appearance of the reconstructed surfaces at large tip-sample distances, if they are incorporated in the missing-row troughs of the substrate. The potassium 4*s* resonance level is then centered energetically well below the Fermi level and has only a small spectral weight at the Fermi level. However, at smaller separations of the tunneling electrodes (≤ 5 Å) tip-sample interactions lead to qualitative changes in the charge-density distribution at the Fermi level of the interacting system. This effect leads to an inversion of the STM image, a phenomenon which is also observed experimentally.

Theoretical calculations have not been performed for the Au(110) surface, but it is suggested that qualitatively similar results would have been obtained. The anticorrugating nature of the tip-sample interaction has theoretically been established for various other clean metal surfaces [Al(111), Al(100), Pd(111), Pd(100) (Ref. 2)]. The transparency of the adsorbed alkali-metal atoms is associated with the fact that they are incorporated in the missing rows and that the alkali-metal-induced wave functions near the Fermi level have antibonding character and are more standing-wave-like. Therefore they do not conduct electrons easily. These are qualitative concepts which can be applied for understanding the imaging of similar surfaces.

ACKNOWLEDGMENT

Financial support by the Deutsche Forschungsgemeinschaft via Sonderforschungsbereich 6 is acknowledged.

*Permanent address: Chemistry Department, University of Sofia, Bulgaria.

†Present address: Technischer Überwachungsverein Bayern, München, Germany.

‡Permanent address: Institut für Oberflächenchemie und Katalyse, Universität Ulm, Germany.

[1]J. Tersoff and D. R. Hamann, Phys. Rev. Lett. **50**, 1998 (1983); Phys. Rev. B **31**, 805 (1985).

[2]G. Doyen, D. Drakova, and M. Scheffler, Phys. Rev. B **47**, 9778 (1993).

[3]N. J. Zheng and I. S. T. Tsong, Phys. Rev. B **41**, 2671 (1990).

[4]S. Ciraci, A. Baratoff, and Inder P. Batra, Phys. Rev. B **41**, 2763 (1990).

[5]J. Wintterlin and R. J. Behm, in *Scanning Tunneling Microscopy I,* edited by H.-J. Güntherodt and R. Wiesendanger, Springer Series in Surface Sciences Vol. 20 (Springer, Berlin, 1992), p. 39.

[6]D. M. Eigler, P. S. Weiss, E. K. Schweizer, and N. D. Lang, Phys. Rev. Lett. **66**, 1189 (1991).

[7]E. Kopatzki and R. J. Behm, Surf. Sci. **245**, 255 (1991).

[8]D. J. Coulman, J. Wintterlin, R. J. Behm, and G. Ertl, Phys. Rev. Lett. **64**, 1761 (1990).

[9]H. Brune, J. Wintterlin, G. Ertl, and R. J. Behm, Europhys. Lett. **13**, 123 (1990).

[10]N. D. Lang, Comments Condens. Matter Phys. **14**, 253 (1989).

[11]R. Schuster, J. V. Barth, G. Ertl, and R. J. Behm, Surf. Sci. Lett. **247**, L229 (1991).

[12]R. Schuster, J. V. Barth, G. Ertl, and R. J. Behm, Phys. Rev. B **44**, 13 689 (1991).

[13]J. Wintterlin, J. Wiechers, H. Brune, T. Gritsch, H. Höfer, and R. J. Behm, Phys. Rev. Lett. **62**, 59 (1989).

[14]P. Häberle and T. Gustafsson, Phys. Rev. B **40**, 8218 (1989).

[15]D. K. Flynn-Sanders, K. D. Jamison, J. V. Barth, J. Wintterlin, P. A. Thiel, G. Ertl, and R. J. Behm, Surf. Sci. **253**, 270 (1991).

[16]W. C. Fan and A. Ignatiev, Phys. Rev. B **38**, 366 (1988).

[17]G. Doyen, E. Koetter, J. Barth, and D. Drakova, in *Basic Concepts and Applications of Scanning Tunneling Microscopy (STM) and Related Techniques,* edited by R. J. Behm, N. Garcia, and H. Rohrer (Kluwer Academic, Dordrecht, 1990), p. 97.

[18]G. Doyen, E. Koetter, J. P. Vigneron, and M. Scheffler, Appl. Phys. A **51**, 281 (1990).

[19]G. Doyen, in *Scanning Tunneling Microscopy III,* edited by H.-J. Güntherodt and R. Wiesendanger, Springer Series in Surface Sciences Vol. 29 (Springer, Berlin, 1993), Chap. 3, p. 23.

[20]V. L. Moruzzi, J. F. Janak, and A. R. Williams, *Calculated Electronic Properties of Metals* (Pergamon, New York, 1978).

[21]J. Hölzl and F. K. Schulte, in *Solid Surface Physics,* edited by G. Höller, Springer Tracts in Modern Physics Vol. 85 (Springer, Berlin, 1979).

[22]B. Woratscheck, W. Sesselmann, J. Küppers, G. Ertl, and H. Haberland, Phys. Rev. Lett. **55**, 1231 (1985).

[23]F. Jensen, F. Besenbacher, E. Lægsgaard, and I. Stensgaard, Phys. Rev. B **41**, 10 233 (1990).

[24]J. Lapujoulade, Y. LeGruër, M. Lefort, Y. Lejay, and E. Maurel, Surf. Sci. **118**, 103 (1982).

[25]G. Binning, H. Rohrer, C. Gerber, and E. Weibel, Surf. Sci. **131**, L379 (1983).

[26]T. Gritsch, D. Coulman, R. J. Behm, and G. Ertl, Surf. Sci. **257**, 297 (1991).

[27]J. K. Gimzewski, R. Berndt, and B. R. Schlittler, Phys. Rev. B **45**, 6844 (1992).

[28]T. Gritsch, Ph.D. thesis, Freie Universität Berlin, 1990.

[29]W. Moritz and D. Wolf, Surf. Sci. **163**, L655 (1985).

[30]J. V. Barth, Ph.D. thesis, Freie Universität Berlin, 1992.

[31]N. D. Lang, Phys. Rev. B **37**, 10 395 (1988).

[32]R. J. Behm, in *Physics and Chemistry of Alkali Metal Adsorption,* edited by H. P. Bonzel, A. M. Bradshaw, and G. Ertl, (Elsevier, New York, 1989), p. 111.

[33]R. Schuster, J. V. Barth, G. Ertl, and R. J. Behm, Phys. Rev. Lett. **69**, 2547 (1992).

[34]R. Schuster, Ph.D. thesis, Freie Universität Berlin, 1992.

[35]J. Wintterlin, R. Schuster, D. J. Coulman, and G. Ertl, J. Vac. Sci. Technol. B **9**, 902 (1991).

[36]D. Drakova, G. Doyen, and R. Hübner, J. Chem. Phys. **89**, 1725 (1988).

[37]K. M. Ho, C. T. Chan, and K. P. Bohnen, Phys. Rev. B **40**, 9978 (1989).

[38]J. V. Barth, R. Schuster, G. Ertl, and R. J. Behm (unpublished).

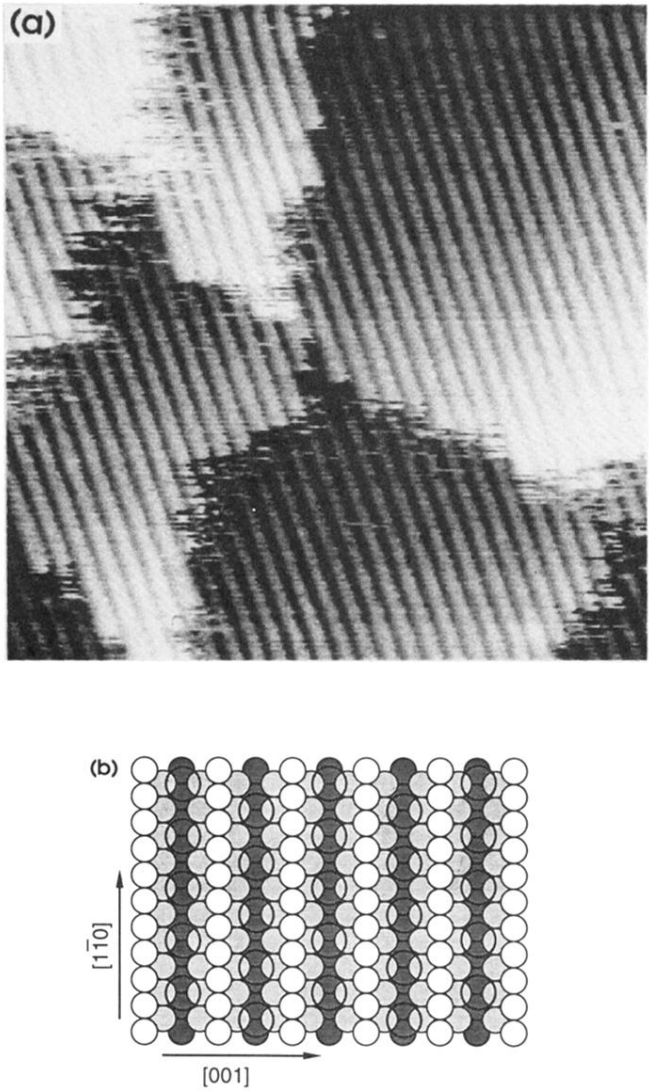

FIG. 10. (a) STM image of the (1×2) missing-row reconstructed K/Cu(110) surface at $\Theta=0.20$. (b) Model for the K-covered (1×2) structure. The symbols are identical with those in Fig. 8.

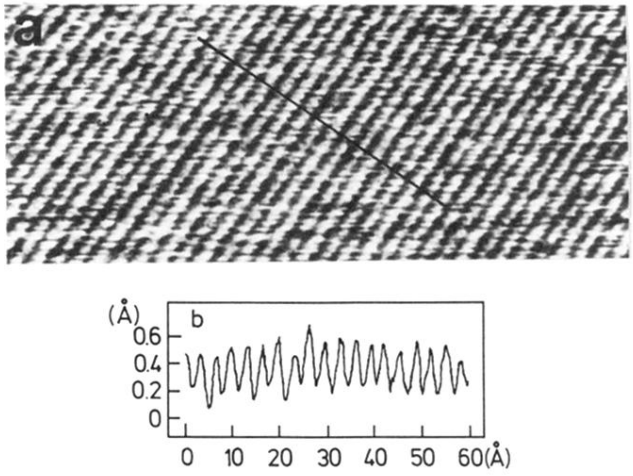

FIG. 1. (a) Experimental STM image of the clean Cu(110) surface. (b) STM contour line along the marked line in (a).

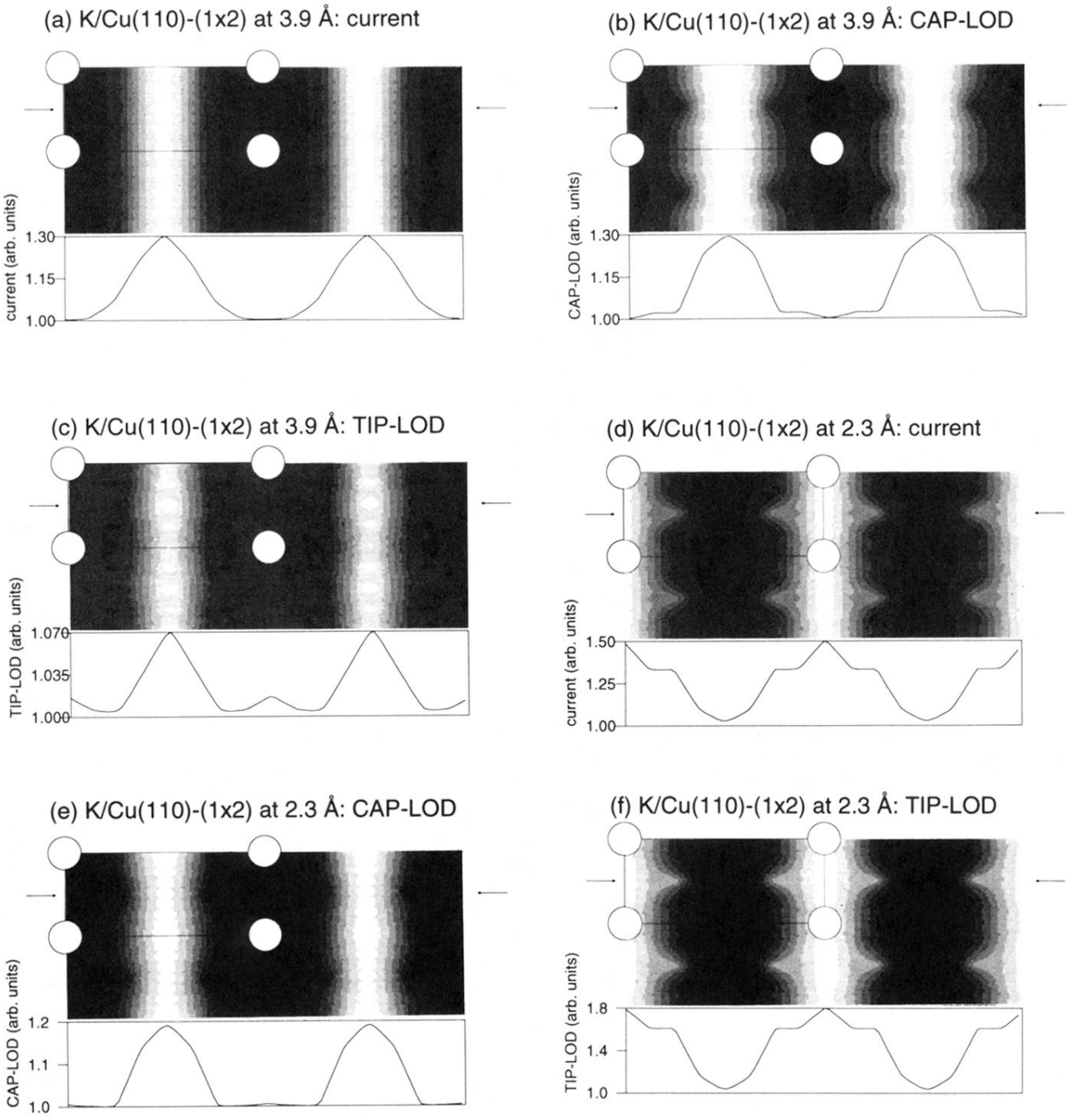

FIG. 11. (a) Calculated variation of the tunnel current across the K-covered Cu(110)-(1×2) missing-row reconstructed surface at a constant height of 3.9 Å above the first layer of K atoms. (b) Variation of CAP-LOD and (c) TIP-LOD across the K-covered Cu(110)-(1×2) missing-row reconstructed surface at a constant height of 3.9 Å above the first layer of K atoms. (d) Variation of the tunnel current across the K-covered Cu(110)-(1×2) missing-row reconstructed surface at a constant height of 2.3 Å above the first layer of K atoms. (e) Variation of CAP-LOD and (f) TIP-LOD across the K-covered Cu(110)-(1×2) missing-row reconstructed surface at a constant height of 2.3 Å above the first layer of K atoms. (The circles indicate the position of the K atoms in the surface unit cell.)

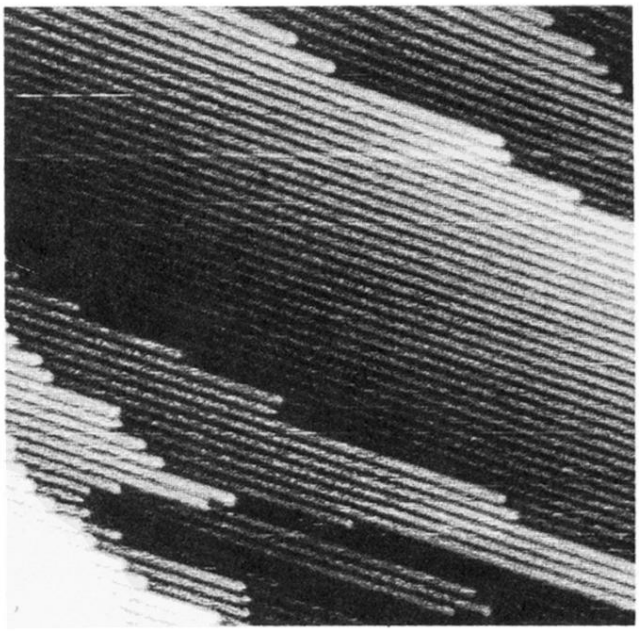

FIG. 12. STM image of Au(110)-(1×2) with a K coverage of 0.15 ML.

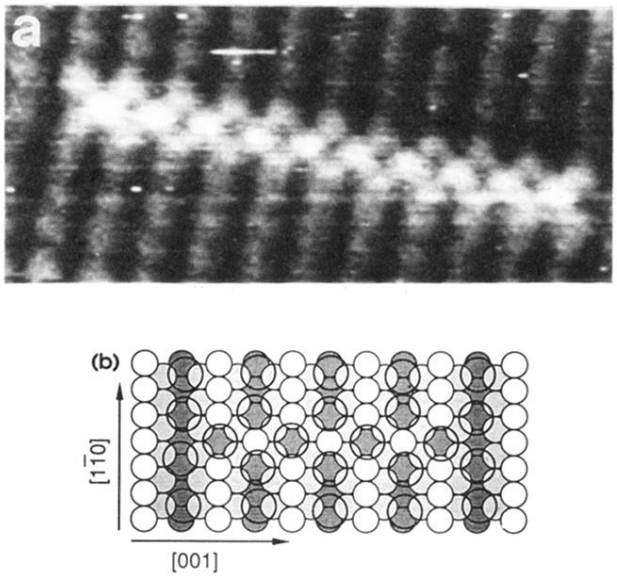

FIG. 13. (a) STM image of Au(110) with a K coverage of 0.32 ML. (b) Model of the $c(2\times2)$ nucleus for K/Au(110). For an explanation of the symbols, see Fig. 8.

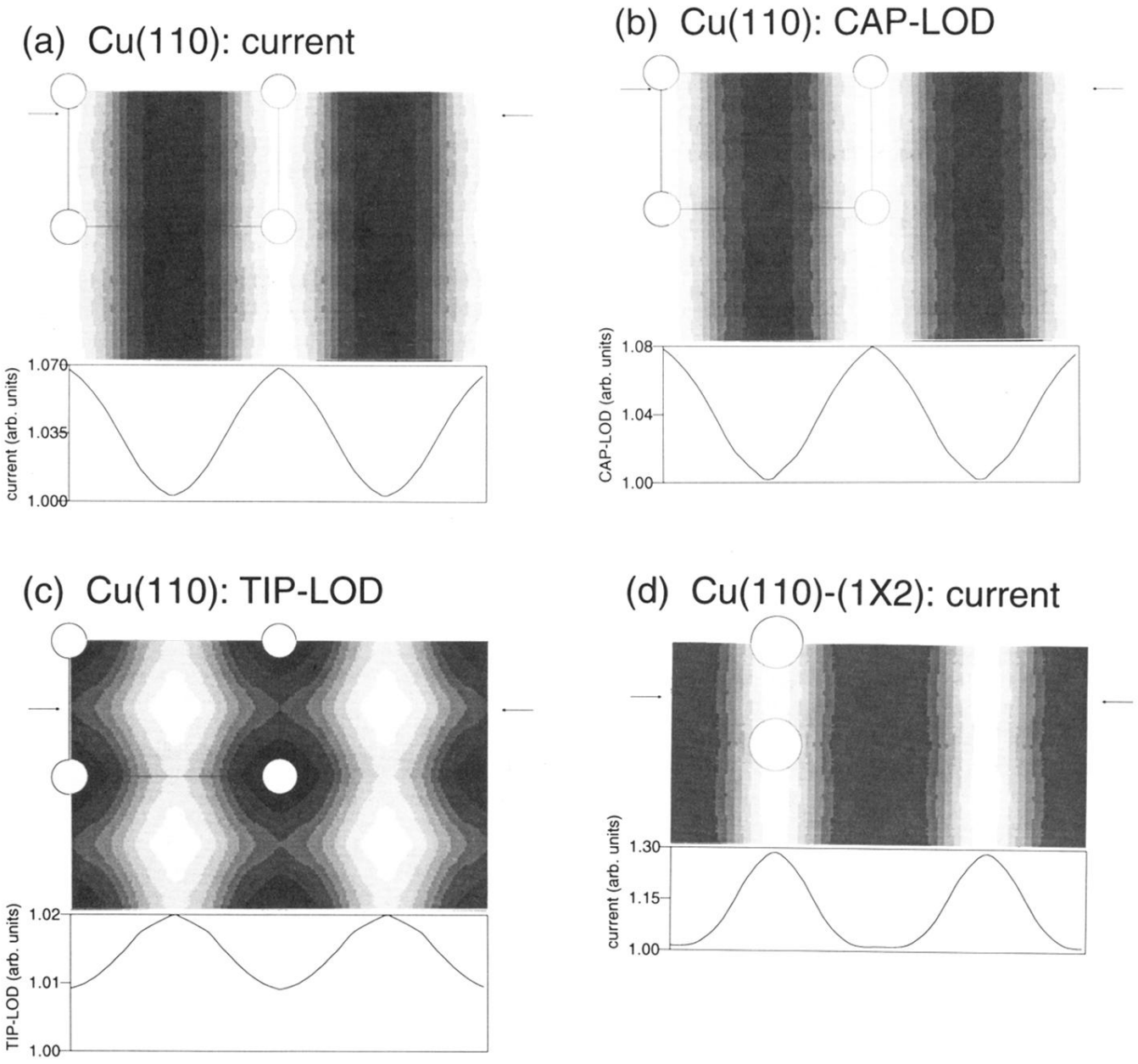

FIG. 2. (a) Gray scale representation of the calculated variation of the total tunneling current parallel to a Cu(110) surface for a tip-sample separation of 3.9 Å. The maximal variation is 7%, as can be seen from the contour line at the bottom of the figure which gives the current along the line connecting the two arrows. The empty circles indicate Cu atoms in the first layer. (b) Lateral variation of the capacitor-projected local density at the Fermi level (CAP-LOD) for Cu(110) at a tip-sample separation of 3.9 Å. (c) Lateral variation of the tip-projected local density at the Fermi level (TIP-LOD) for Cu(110) at a tip-sample separation of 3.9 Å. (d) Variation of the total tunnel current parallel to a Cu(110)-(1×2) missing-row reconstructed surface at a constant height of 3.9 Å above the first layer of Cu atoms. The maximum variation is approximately 30%. The empty circles indicate the positions of the Cu atoms in the surface unit cell.

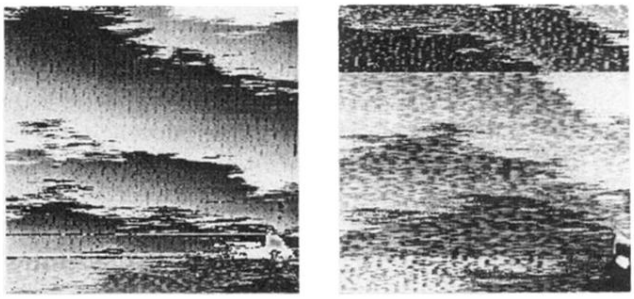

FIG. 9. STM images of the local reconstruction of Cs/Cu(110) at $\Theta = 0.05$ in different imaging modes of the tip. Both images show the same surface area. In the lower part of the left image and in the upper part of the right image the state of the tip changed.